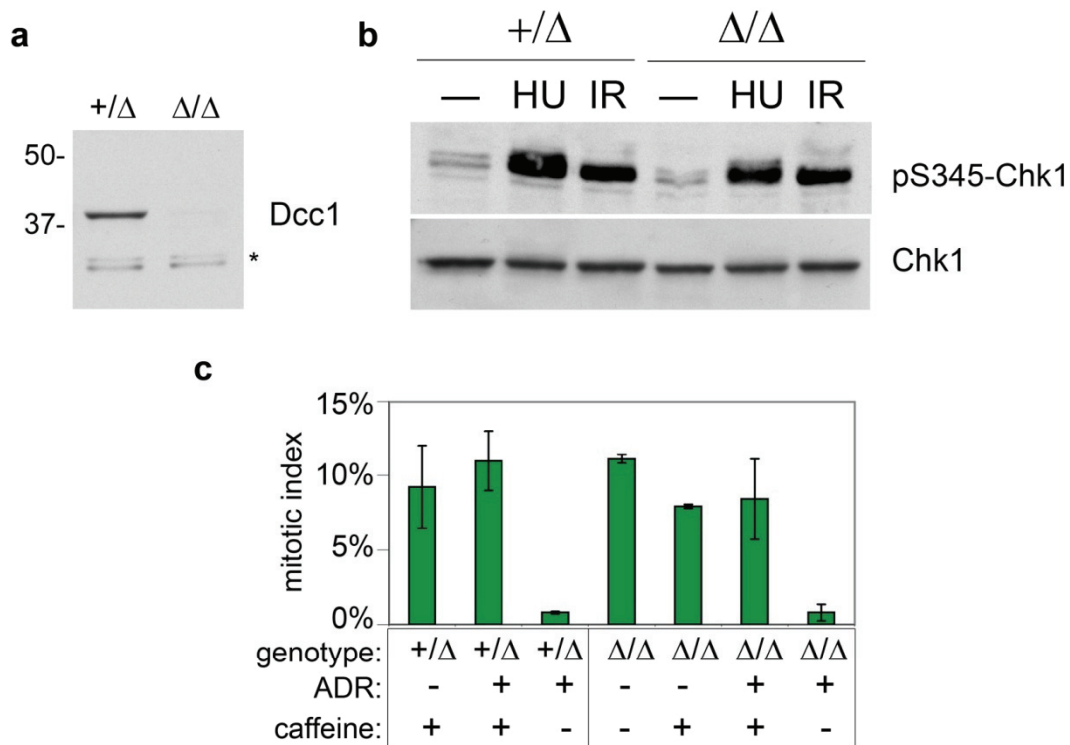
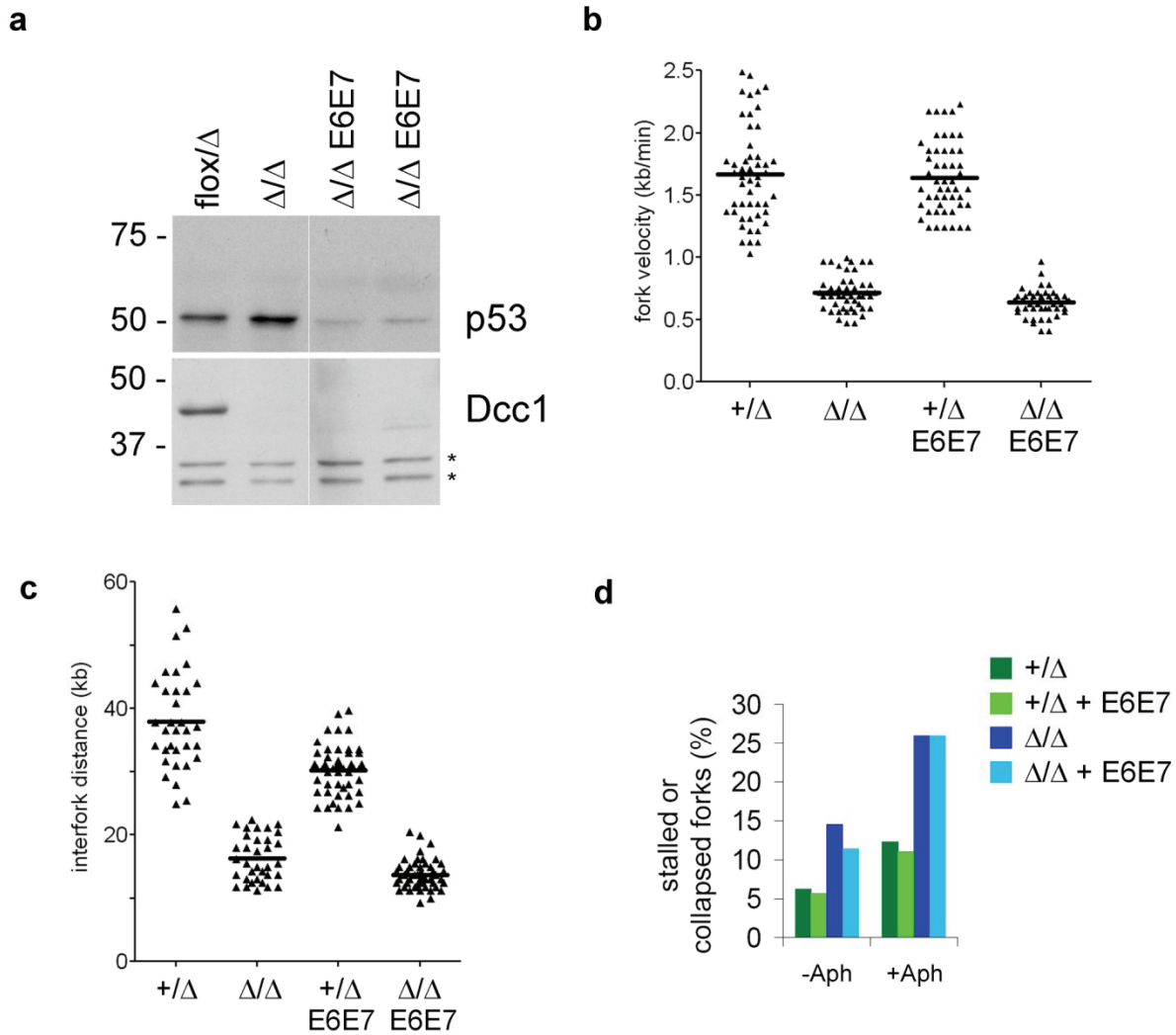


Supplementary Figure 1. Conditional deletion of the *DCC1* locus in human cells.

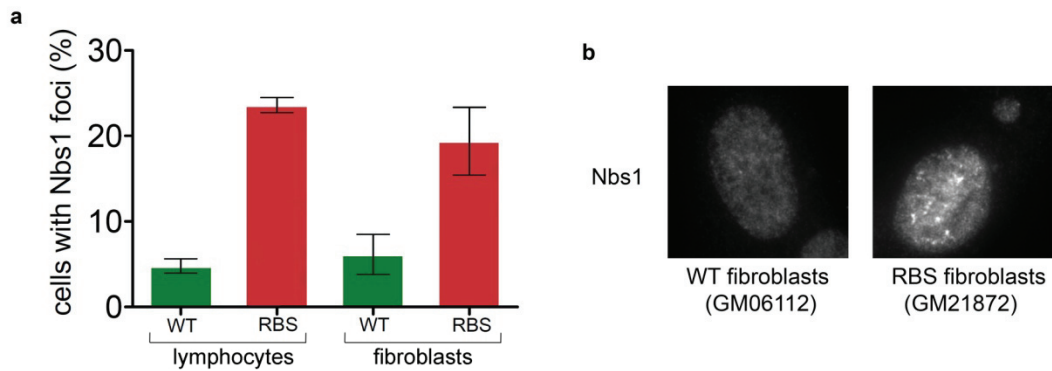
a, Structure of the adeno-associated virus (AAV) vectors used to mutate both alleles of *DCC1* in human retinal pigment epithelial cells. Filled triangles and open circles denote *loxP* and *FRT* sites, respectively. **b**, Genomic DNAs from cells of the indicated genotypes were digested with *SacI*, resolved on a 0.8% Tris-acetate-EDTA agarose gel, and transferred to a membrane support (Bio-Rad). The blot was hybridized with the [³²P]-labeled probe in Fig. 1a and exposed to film. The *flox** notation indicates the first targeted allele prior to removal of the *neo^R* cassette with FLP recombinase. Bands corresponding to the *wt* (3 kb), *flox** (4.8 kb), *flox* (3.2 kb), and Δ alleles (constitutive 4.5 kb, Cre-dependent 2.7 kb) were observed as expected.



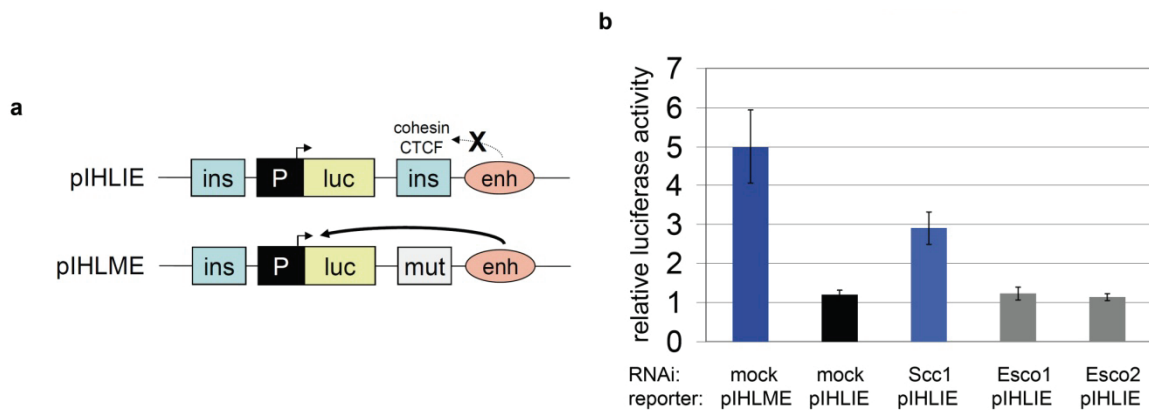
Supplementary Figure 2. RFC^{Ctf18}-deficient cells activate Chk1 in response to DNA damage or replication stress. **a**, Cells of the indicated genotypes were generated by AdCre infection as in Fig. 1. Immunoblot demonstrates depletion of Dcc1. Asterisk marks nonspecific bands, used here to confirm equivalent loading. **b**, Cells were treated with 1 mM hydroxyurea (HU) for 5 hours, irradiated with 10 Gy ionizing radiation (IR) and collected 1 hour later, or left untreated as a control. Lysates were resolved by SDS-PAGE and immunoblotted with antibodies recognizing serine 345 phosphorylation (top panel) or total Chk1 (bottom panel). **c**, G2/M checkpoint assay. First, where indicated, checkpoint deficiency was induced by a 30 minute pretreatment with 5 mM caffeine. Next, 0.5 μM adriamycin was added to the indicated cultures to induce DNA damage. 90 minutes later, 0.2 μg/ml nocodazole was added to all cultures to trap cells entering mitosis. After 6 hours, cells were harvested, fixed and stained with Hoechst 33258, and viewed by fluorescence microscopy to determine the mitotic index. At least 600 cells were counted for each data point.



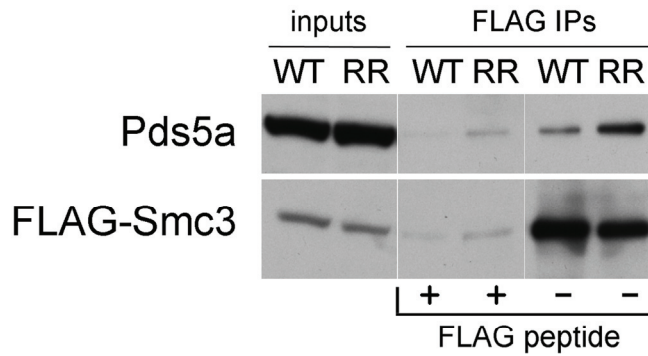
Supplementary Figure 3. Analysis of replication fork dynamics in non-senescent cells. Human papillomavirus E6 and E7 proteins were expressed in *DCC1^{flox/Δ}* cells via retroviral transduction. RFC^{Ctf18} inactivation was initiated by infection with AdCre. **a**, Downregulation of p53 and Dcc1 was confirmed by immunoblotting. **b-d**, Replication fork velocities (**b**), intervals between adjacent forks (**c**), and frequency of fork arrest with or without intervening treatment with 10 μ M aphidicolin (**d**) were determined.



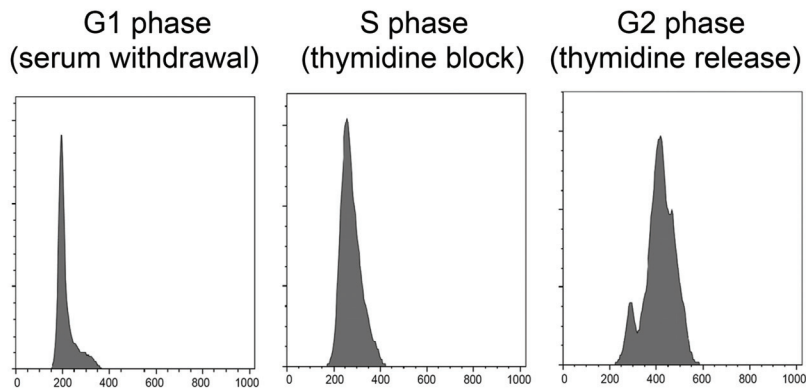
Supplementary Figure 4. RBS cells accumulate spontaneous DNA damage. EBV-immortalized lymphoblasts and fibroblasts from two normal donors and two unrelated RBS patients were fixed and stained with antibodies to Nbs1. **a**, Frequency of nuclear Nbs1 foci was determined from at least 100 cells per sample (n = 3). **b**, Nbs1 staining patterns in WT and RBS fibroblasts.



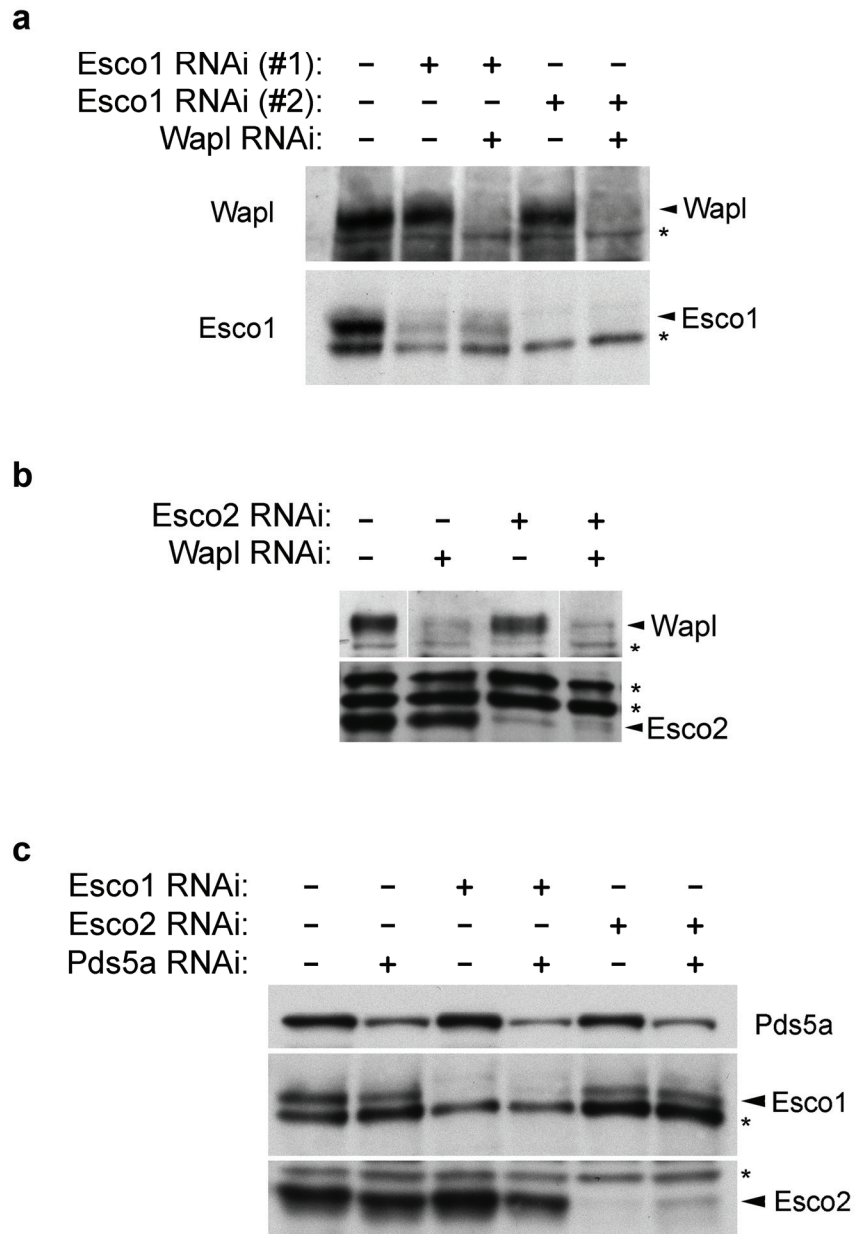
Supplementary Figure 5. Cohesin acetyltransferases are dispensable for gene insulation. **a**, Structure of the insulator reporter constructs (ref. 35). In pIHLIE, insulators (ins) from the *H19* locus recruit cohesin and CTCF, preventing enhancer-dependent activation of the firefly luciferase reporter. In pIHLME, the 3' insulator's CTCF/cohesin-binding sites are mutated (mut), disabling its function. **b**, HeLa cells transfected with siRNAs specific for Sccl, Esco1, or Esco2. 24 hours later, cells were treated with thymidine overnight to induce S phase arrest. After thymidine washout, cells were again transfected with pIHLIE or pIHLME, together with a Renilla luciferase plasmid as a transfection control, and then synchronized in G2 via a second thymidine block and release. The ratio of firefly to Renilla luciferase activities was determined in cell lysates from each condition (n = 3; error bars denote standard deviation).



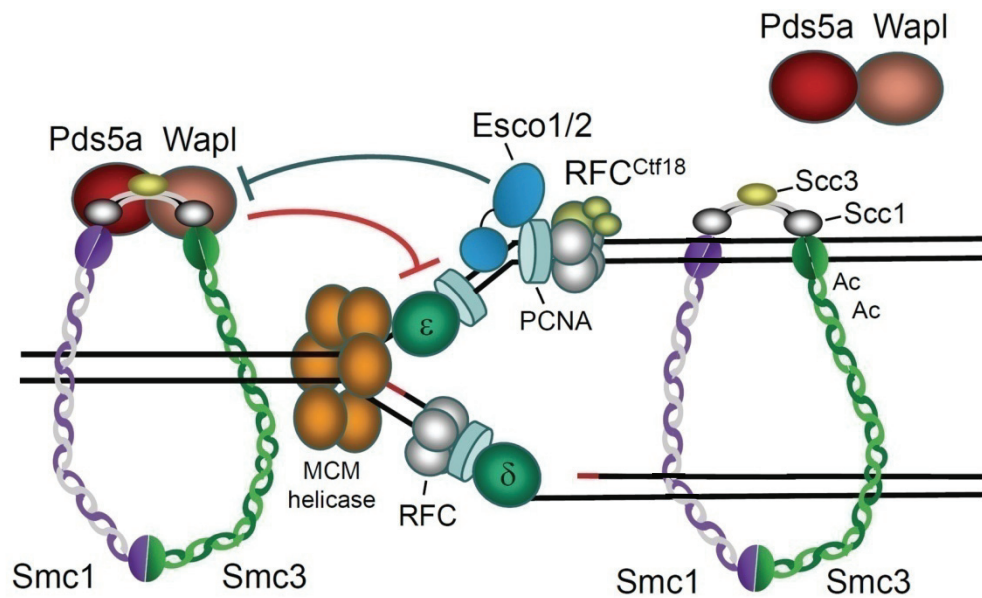
Supplementary Figure 6. Mutating Smc3's acetyl-accepting lysines to arginine stabilizes Pds5a binding. HEK293 cells were transiently transfected with plasmids expressing FLAG-tagged wildtype (WT) or K105R,K106R (RR) mutant forms of Smc3. FLAG-Smc3 associated proteins were immunoprecipitated and analyzed by Western blotting as in Fig. 4a.



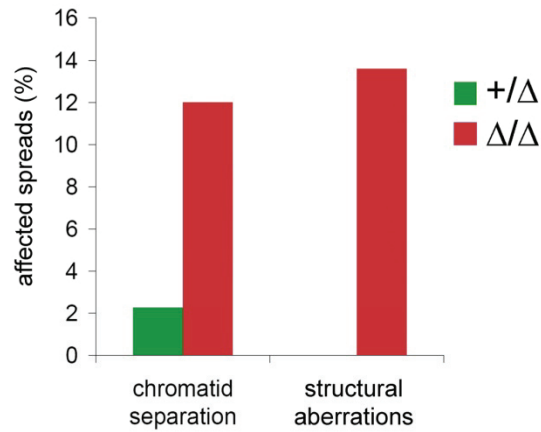
Supplementary Figure 7. FACS analysis of cell cycle synchrony. Cell populations used in Fig. 4b were analyzed by flow cytometry.



Supplementary Figure 8. Depletion of Esco1, Esco2, Pds5a and Wapl via RNAi. Lysates from siRNA-transfected HeLa cells in Fig. 4e were resolved by SDS-PAGE and immunoblotted with the indicated antibodies. Asterisks denote non-specific bands.



Supplementary Figure 9. A model for coordination of cohesin acetylation and replication fork progression via the Wapl/Pds5a complex. During early S phase, replication forks encounter cohesin rings that are predominantly unacetylated and thus bound tightly to Wapl and Pds5a, creating a physical impediment to chain elongation. Through interactions with RFC^{Ctf18}-loaded PCNA and/or RFC^{Ctf18} itself, Esco1 and Esco2 are stimulated to acetylate Smc3 on two conserved lysine residues. This modification disrupts the interaction between cohesin and the Wapl/Pds5a subcomplex and may place the cohesin ring in an open conformation that allows the replisome to pass through it. As cohesin slides or is reloaded onto the nascent sister DNAs, its cohesive activity could provide a positive cue for replication restart, similar to the role proposed for hemicatenanes during template switching.



Supplementary Figure 10. Cohesion loss and structural aberrations in senescence-proficient *DCC1*^{Δ/Δ} cells. Cells of the indicated genotypes were infected with AdCre in the absence of E6 and E7 co-expression. At passage 1, cultures were treated with a low dose of aphidicolin (0.3 μM) for 15 hours and then processed for metaphase spreads. The frequency of separated chromatids or structurally aberrant chromosomes (e.g., gaps and multiradials) was scored from 100 spreads each.

Gene Symbol	Ensembl ID	fold change	
		Scc1 RNAi	Smc3 AA/WT
<i>MMP28</i>	ENSG00000129270	0.40	0.99
<i>SLC35C2</i>	ENSG00000080189	0.70	0.99
<i>CRTAP</i>	ENSG00000170275	0.75	0.99
<i>CAST</i>	ENSG00000153113	1.30	0.97
<i>TNPO1</i>	ENSG00000083312	1.30	1.08
<i>PTK2</i>	ENSG00000169398	1.40	1.00
<i>USP25</i>	ENSG00000155313	1.40	0.94
<i>ATG5</i>	ENSG00000057663	1.45	0.99
<i>TLK2</i>	ENSG00000146872	1.45	1.08
<i>TOP2B</i>	ENSG00000077097	1.50	1.02
<i>TRMT11</i>	ENSG00000066651	1.50	1.19
<i>VTA1</i>	ENSG00000009844	1.50	1.08
<i>YOD1</i>	ENSG00000180667	1.55	1.03
<i>C10orf4</i>	ENSG00000148690	1.60	0.93
<i>ELF2</i>	ENSG00000109381	1.65	1.04
<i>EXOC6</i>	ENSG00000138190	1.65	1.03
<i>GRINL1A</i>	ENSG00000137878	1.65	0.91
<i>SFRS12</i>	ENSG00000153914	1.70	0.96
<i>GOLGA8A</i>	ENSG00000175265	1.80	1.13
<i>JMJD1C</i>	ENSG00000171988	1.80	1.03
<i>MKLN1</i>	ENSG00000128585	1.80	0.91
<i>PFDN4</i>	ENSG00000101132	1.80	0.92
<i>MEF2A</i>	ENSG00000068305	1.85	1.08
<i>AKAP2</i>	ENSG00000157654	1.90	0.91
<i>AGTPBP1</i>	ENSG00000135049	2.00	0.97
<i>SEPT7</i>	ENSG00000122545	2.00	0.96
<i>ASPH</i>	ENSG00000198363	2.10	0.93
<i>CAMSAP1L1</i>	ENSG00000118200	2.10	1.13
<i>OXR1</i>	ENSG00000164830	2.15	0.97
<i>PIK3R3</i>	ENSG00000117461	2.15	1.33
<i>FUT8</i>	ENSG00000033170	2.35	1.07
<i>STK3</i>	ENSG00000104375	2.50	1.18
<i>RND3</i>	ENSG00000115963	2.75	1.07
<i>PLEKHA5</i>	ENSG00000052126	2.90	0.96
<i>ALCAM</i>	ENSG00000170017	4.15	1.07
<i>REEP3</i>	ENSG00000165476	4.25	1.11

Supplementary Table 1. Expression analysis of cohesin-regulated genes in cells with wildtype (WT) or non-acetylatable (AA) Smc3. Total RNA was harvested from cells induced to express Smc3^{WT} or Smc3^{AA}. Labeled cRNA was prepared from two independent biological replicates and hybridized to HumanRef-8 BeadChips (Illumina). Fold changes (AA/WT) were evaluated against a previously reported signature of 36 genes that are positioned near cohesin-binding sites and either upregulated (33) or downregulated (3) after Scc1 RNAi (ref. 5). Fold changes ≥ 1.3 and ≤ 0.75 are highlighted. For the AA/WT comparison, no change reached statistical significance after unpaired t-test and Benjamini-Hochberg FDR correction.